e-ISSN 2320 –7876 www.ijfans.org
Vol.11, Iss.9, Dec 2022

Research Paper

Sol-gel synthesis and physical-chemical characterization studies of magnetic iron molybdate nanoparticles

B. Kavitha[1,*], G. Padma Priya[1]
[1] Department of Chemistry, Faculty of Arts and Science,
Bharath Institute of Higher Education and Research (BIHER),
Chennai – 600073, Tamil Nadu, India
***Corresponding Author Email: kaviselvan78@gmail.com** (B. Kavitha)

Address for Correspondence

B. Kavitha[1,*], G. Padma Priya[1]
[1] Department of Chemistry, Faculty of Arts and Science,
Bharath Institute of Higher Education and Research (BIHER),
Chennai – 600073, Tamil Nadu, India
***Corresponding Author Email: kaviselvan78@gmail.com** (B. Kavitha)

Abstract

Magnetic nature of iron molybdate nanoparticles were successfully synthesized using metal nitrates, citric acid and ethyl cellulose by a simple sol-gel method. Structural, morphological, optical and magnetic properties of the iron oxide nanoparticles were characterized by powder XRD, FT-IR) spectra, HR-SEM, EDX, UV-Visible DRS, PL spectra and VSM. Powder XRD results indicated that the resultant iron oxide nanoparticles was pure single phase crystalline with monoclinic structure. FT-IR spectra indicate the type of bonds between Fe and O. HR-SEM images shows that the morphology of iron oxide consists with well-defined nanoparticles structure. VSM results showed ferromagnetic behavior.

Keywords: Sol-gel synthesis; nanoparticles Magnetic properties.

1. Introduction

Nano-structured magnetic materials have attracted considerable attention in recent years due to their unusual physical and chemical properties than that of their same bulk materials. It is well known that nano-sized particles, because of their small size and high surface area, display

many unique properties such as electrical, optical, magnetic and photocatalytic properties [1-8]. Nano-sized particles exhibits interesting applications in biology, catalysis, sensors, ceramics, mechanics and electronics fields [9-15]. As a family of important functional magnetic materials, metal molybdates have been widely used in photoluminescence, microwave applications, optical fibers, scintillator materials, humidity sensors and electro-catalysis [16-22]. Among many metal molybdates, magnetic nature of iron molybdate nanoparticles is a particularly efficient catalyst for the oxidation of methanol to formaldehyde and exhibits very interesting magnetic properties [23, 24]. As catalysts, magnetic nature of iron molybdate nanoparticles are used industrially for the oxidation of various alcohols [25]. The effectiveness of these catalytic activities generally depends heavily on particle size and surface area, which in turn depend on processing. Most studies to date have been on bulk materials produced by solid-state synthesis. Several methods such as solid-state reaction, sol-gel process, co-precipitation, hydrothermal, thermal [26-30] techniques have been used to produce nanoparticles, showing the improved catalytic abilities.

In this work, we attempt to synthesize magnetic nature of iron molybdate nanoparticles by a simple sol-gel method using ethyl cellulose as surfactant. Compared with the above conventional methods, sol-gel technique exhibits many advantages, such as low process temperature, high control of purity, composition, microstructure and textural properties of the final products [31-36]. Ethyl cellulose is a derivative of cellulose in which some of the hydroxyl groups on the repeating glucose units are converted into ethyl ether groups. The number of ethyl groups can vary depending on the manufacturer. Ethyl cellulose contains a hydroxyl group in its individual unit, which plays an important role in the dispersion process of magnetic nature of iron molybdate nanoparticles. This hydroxyl group forms an ester linkage with Citric Acid which forms big polymeric structure which traps the metal salts & water and thus prevents the agglomeration of particles. The photocatalytic degradation of different toxic compounds, such as organic or inorganic pollutants, eliminated through photochemical reaction by using TiO_2 photocatalysts, has been widely studied.

However, hydrothermal procedures usually require a long reaction time. A facile and fast solution-based procedure is highly desired for the preparation of magnetic nature of iron molybdate nanoparticles. To the best of our knowledge, there has been no report on the

preparation of such magnetic nature of iron molybdate nanoparticles by ethyl cellulose supported sol-gel method. By controlling the experimental parameters, such as the amount of citric acid and ethyl cellulose, reaction time, temperature and iron source, novel magnetic nature of iron molybdate nanoparticles have been successfully fabricated. Moreover, magnetic and photocatalytic properties of the obtained samples were studied.

2. Experimental techniques

2.1 Materials and methods

All the chemicals used in this study were of analytical grade obtained from Merck, India and were used as received without further purification. Ammonium molybdate ($(NH_4)_6\ Mo_7O_{24}.\ 4H_2O$), ferric nitrate ($Fe\ (NO_3)_3.9\ H_2O$), citric acid and ethyl cellulose were used for this sol-gel method. Ethyl cellulose powders were sprinkled slowly into de-ionized water under continuous stirring to avoid clumping of the material in water. Ferric nitrate and ammonium molybdate in stoichiometric ratio and citric acid were dissolved in deionized water separately. These solutions were added to ethyl cellulose solution at 50°C to form sol. This sol is then heated slowly to 90°C under constant stirring to obtain a wet gel. Then the gel product was calcined at 650 °C for 2 h. It was ground in a mortar to form a final product of fine powder.

2.2. Characterization techniques

The characterization of the obtained $Fe_2(MoO_4)_3$ powder were conducted by using various techniques to verify the phase formation, crystallite size, distribution and to explore other parameters of interest. The structural characterization of $Fe_2(MoO_4)_3$ nanorods (NRs) were performed using Rigaku Ultima X-ray diffractometer equipped with Cu-Kα radiation (λ =1.5418 Å). The surface functional groups were analyzed by Perkin Elmer FT-IR spectrometer. Morphological studies and energy dispersive X-ray analysis (EDX) of iron molybdate nanoparticles have been performed with a Jeol JSM6360 high resolution scanning electron microscopy (HR-SEM). UV-Visible diffuse reflectance spectrum (DRS) was recorded using Cary100 UV-Visible spectrophotometer to estimate their band gap energy (E_g). Photoluminescence (PL) properties were recorded at room temperature using Varian Cary Eclipse Fluorescence Spectrophotometer. Magnetic measurements were carried out at room

temperature using a PMC MicroMag 3900 model vibrating sample magnetometer equipped with 1 Tesla magnet.

3. Results and Discussion

3.1 Structural analysis

The structural and phase analysis of the samples were characterized by powder X-ray diffraction (XRD) pattern and is shown in Figure 1. All the diffraction peaks could be indexed to monoclinic magnetic nature of iron molybdate nanoparticles, which is in good agreement with the literature values (JCPDS file Card No. 35-0183) [26]. No other impurity peak was detected. The very high peak intensity suggests that the material is highly crystalline. This indicates the complete transformation of the precursor into magnetic nature of iron molybdate nanoparticles. The average crystallite size of iron molybdate nanoparticles was calculated using Debye Scherrer formula given in Eq. (2):

$$L = \frac{0.89\,\lambda}{\beta \cos\theta} \qquad \text{---- (2)}$$

where L is the crystallite size, λ , the X-ray wavelength, θ, the Bragg diffraction angle and β, the full width at half maximum (FWHM). The average crystallite size 'L' calculated from the diffraction peaks was found to be around 44-55 nm.

The lattice parameter of iron molybdate nanoparticles was calculated using the formula given in Eq. (3):

$$\sin^2\theta = \frac{\lambda^2}{4}\left[\frac{4}{3}\left(\frac{h^2 + hk + k^2}{a^2}\right) + \frac{l^2}{c^2}\right] \qquad \text{---- (3)}$$

where θ is the diffraction angle, λ, the incident wavelength (λ = 0.1540 nm), h, k, and l are Miller's indices. The calculated lattice parameter was found to be a = 15.74 Å, b = 9.25 Å, and c = 18.21 Å, which is in good agreement with the JCPDS file Card No. 35-0183. Similar values (a = 15.72 Å, b = 9.24 Å, and c = 18.22 Å) has been reported earlier by Zhang et al. [26].

e-ISSN 2320 –7876 www.ijfans.org
Research Paper
Vol.11, Iss.9, Dec 2022

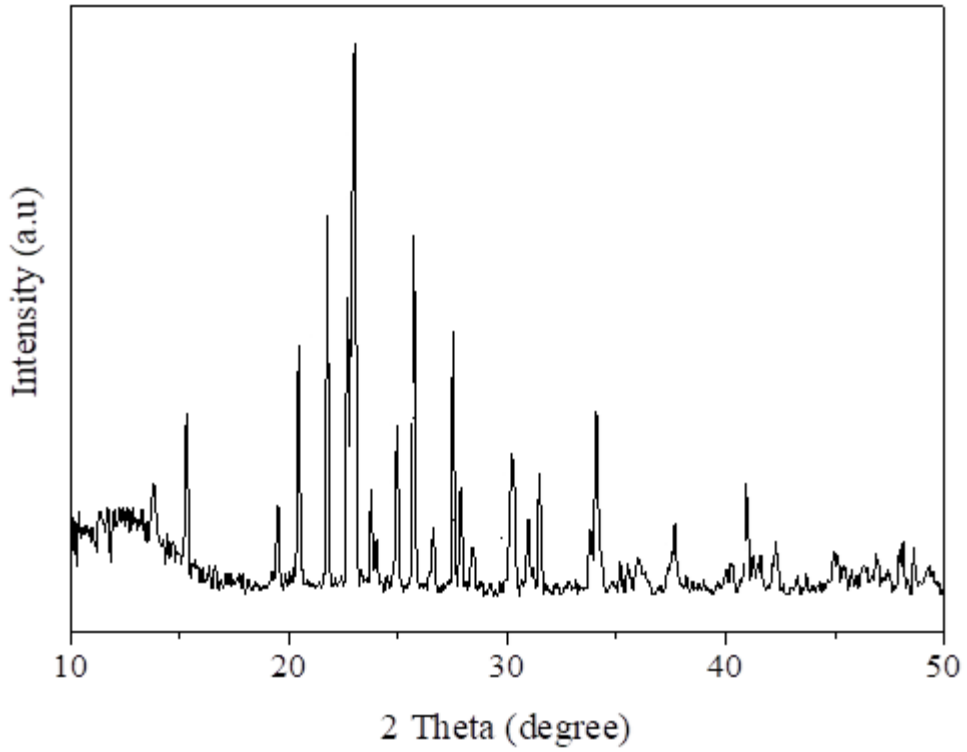

Fig. 1. Powder XRD pattern of iron molybdate nanoparticles.

3.2 FT-IR spectral analysis

Figure 2 shows the FT-IR spectra of iron molybdate nanoparticles. FT-IR spectra contain a broad band between ~ 3200 and ~ 3400 cm^{-1} due to the O-H stretching mode [36]. Furthermore bands related to C=O and C-O stretching modes that appear at ~1723 and ~1042 cm^{-1}, respectively, due to the ester groups formed [37]. The spectra of $Fe_2(MoO_4)_3$ powders shows absorption bands between ~1000 and 1120 cm^{-1} is mainly due to Mo=O stretching vibration. A peak at 827 cm^{-1} is attributed to Mo(VI)-O tetrahedral stretching and peak at 656 cm^{-1} corresponds to Fe(III)-O octahedral stretching vibration. The sharpness of these bands is correlated to the high degree of crystallinity of the iron molybdate nanoparticles.

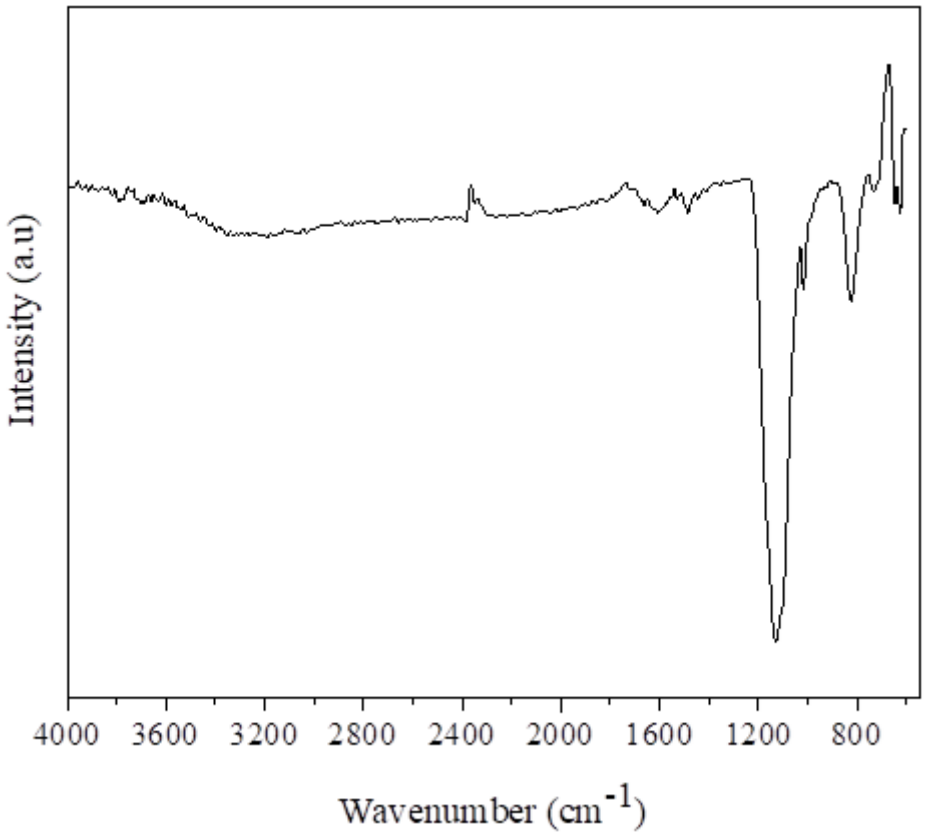

Fig. 2. FTIR spectra of iron molybdate nanoparticles.

3.3. SEM studies

The nanostructure and surface morphology of the as-prepared iron molybdate nanoparticles was examined by high resolution scanning electron microscope (HR-SEM) analysis. Figure 3 shows the HR-SEM images of iron molybdate nanoparticles, which clearly shows the nanoparticles consisting of agglomerated particles. The agglomeration of the particles with nanoparticles structure may be due to the magnetic nature of the samples. In this sol-gel method the crystal formation is due to the stable nuclei via ion-by-ion addition and unit replication. The formation of rods-like structure may be due the agglomeration and attachment of the nano-crystals. Also, the layer-by-layer self-assembled nano-particles, which lead to the formation of rod-like iron molybdate nanoparticles.

e-ISSN 2320 –7876 www.ijfans.org
Vol.11, Iss.9, Dec 2022

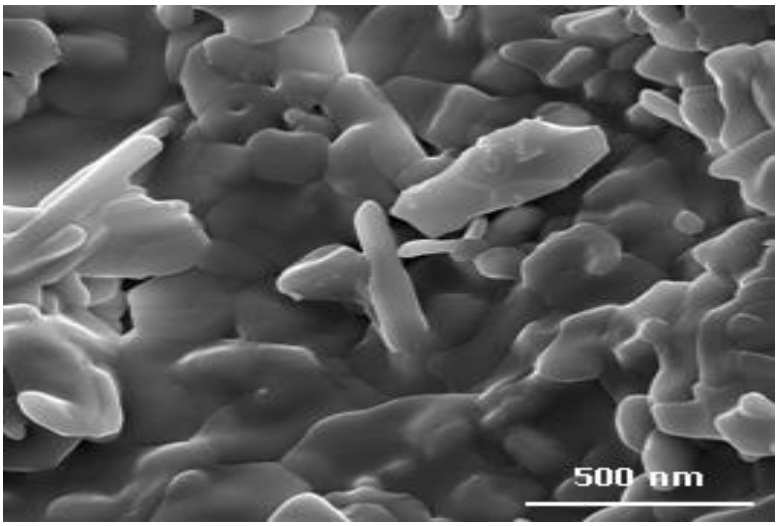

Fig. 3. SEM images of iron molybdate nanoparticles.

3.4. TEM studies

Fig. 4 shows the HR-TEM images of iron molybdate nanoparticles with diameter ranging from 26-50 nm. It is obvious that the sphere-like nanoparticles are uniform in size, which is consistent with the average crystallite size obtained from the peak broadening in XRD. Fig. 4 inset shows the selected area electron diffraction pattern (SAED) of iron molybdate nanoparticles, which implies that the as-prepared samples are single crystalline in nature. SAED results show spotty ring characteristic of small crystallites of spinel ferrite nanostructure without any additional diffraction spots and rings of secondary phases corresponding to the magnesium, nickel and iron oxides were observed.

e-ISSN 2320 –7876 www.ijfans.org
Vol.11, Iss.9, Dec 2022

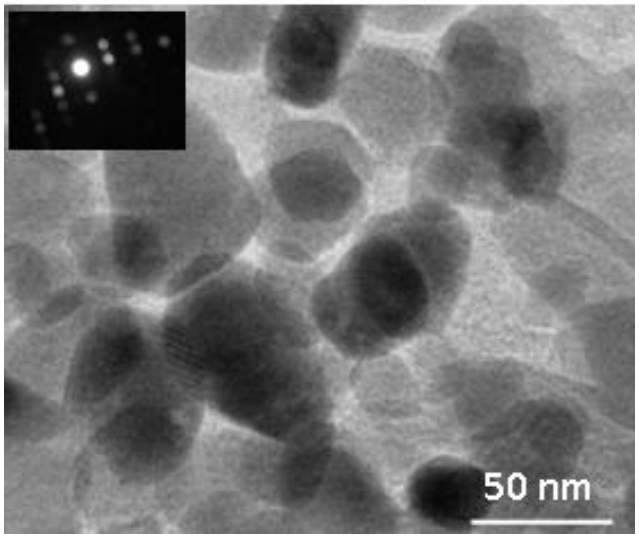

Fig. 4. TEM images of iron molybdate nanoparticles.

3.5. Energy dispersive X-ray (EDX) analysis

Figure 5 shows the EDX spectra of iron molybdate nanoparticles. EDX results showed the presence of Fe, Mo and O by the appearance of Fe, Mo and O peaks without any other characteristic peaks. Hence, the results are a definitive evidence to suggest that the prepared sample does not contain any other element and are indeed free from other impurities.

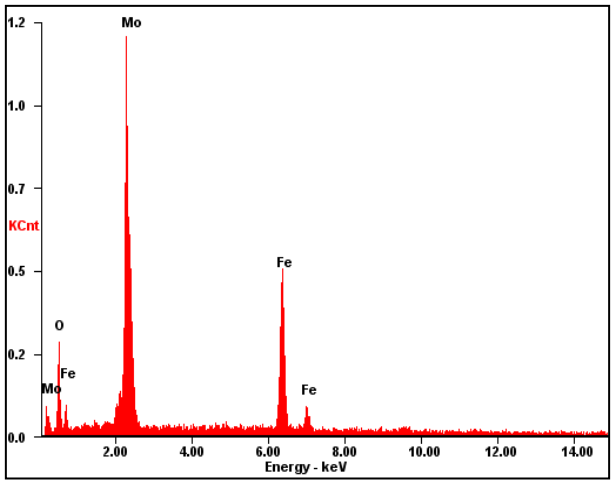

Fig. 5. EDX spectra of iron molybdate nanoparticles.

e-ISSN 2320 –7876 www.ijfans.org
Research Paper
Vol.11, Iss.9, Dec 2022

3.6. UV-Visible DRS spectral studies

The UV-Visible diffuse reflectance spectra (DRS) of nano-crystalline iron molybdate nanoparticles is shown in Figure 6, and the absorption in the UV region at 320 nm is significantly stronger than absorption in the visible region at 530 nm. The broad absorption band centered at 260 nm has been attributed to the O^{2-} to Mo^{6+} charge transfer of the isolated MoO_4 sites [31, 32].

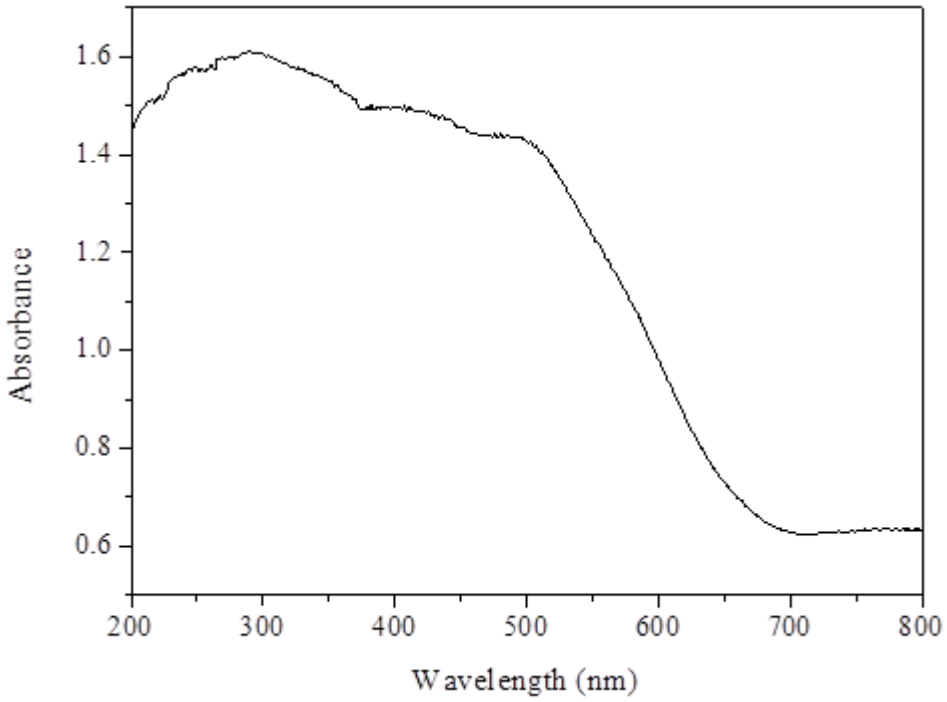

Fig. 6. UV-Visible diffuse reflectance spectra of iron molybdate nanoparticles.

3.6 Magnetic properties

Fig. 7 show the magnetic hysteresis (M-H) loop of the synthesized product with the field sweeping from -10 to +10 kOe at room temperature. The obtained monoclinic iron molybdate nanoparticles particles show ferromagnetic behavior. Magnetic iron molybdate nanoparticles are important magnetic materials, and many efforts have been made to control the size of nanoparticles because of its particle size dependent magnetic properties. The magnetic properties of the iron molybdate nanoparticles are similar to the earlier reported results [33]. The

remarkable ferromagnetic behavior with relatively high saturation magnetization (M_s) of iron molybdate nanoparticles by sol-gel method than that of other methods, which may be due to the synthesis route and its conditions, type of the precursors, calcinations, etc.

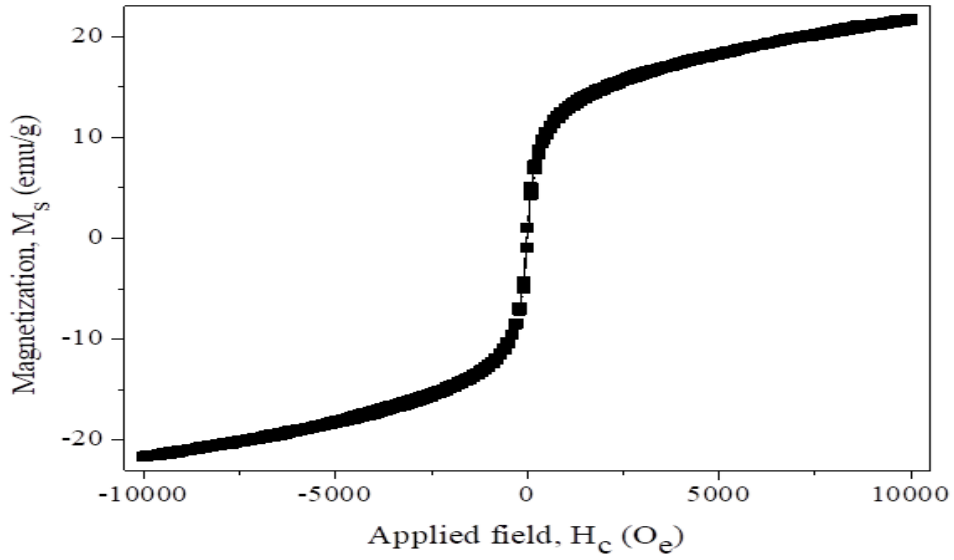

Fig. 7. VSM studies of iron molybdate nanoparticles.

4. Conclusions

Magnetic nature of iron molybdate nanoparticles were successfully synthesized by a simple sol-gel method using ethyl cellulose as surfactant. XRD results indicated that pure single phase crystalline with monoclinic structure of iron molybdate nanoparticles. HR-SEM images show that the morphology of the sample consists with well-defined nanoparticles structure with agglomeration. VSM results showed ferromagnetic behavior. Magnetic nature of iron molybdate nanoparticles may find applications in water pollution control. Compared to other synthetic methods, sol-gel method is a facile, low-cost pathway to novel iron molybdate nanoparticles.

References

[1]. M. A. Almessiere, Y. Slimani, H. Güngüneş, K. A. Demir, Z. Tatiana, T. Sergei, T. Alex, A. Manikandan, A. Fatimah, A. Baykal, Influence of Dy^{3+} ions on microstructure, magnetic, electrical and microwave properties of $[Ni_{0.4}Cu_{0.2}Zn_{0.4}](Fe_{2-x}Dy_x)O_4$ ($0.00<x<0.04$) spinel ferrites, ACS Omega, 6 (2021) 10266-10280.

[2]. P. Annie Vinosha, A. Manikandan, A. Christy Preetha, A. Dinesh, Y. Slimani, M.A. Almessiere, A. Baykal, Belina Xavier, G. Francisco Nirmala, Review on recent advances of synthesis, magnetic properties and water treatment applications of cobalt ferrite nanoparticles and nanocomposites, Journal of Superconductivity and Novel Magnetism, 34 (2021) 995–1018.

[3]. K. Elayakumar, A. Manikandan, A. Dinesh, K. Thanrasu, K. Kanmani Raja, R. Thilak Kumar, Y. Slimani, S. K. Jaganathan, A. Baykal, Enhanced magnetic property and antibacterial biomedical activity of Ce^{3+} doped $CuFe_2O_4$ spinel nanoparticles synthesized by sol-gel method, J. Magn. Magn. Mater. 478 (2019) 140–147.

[4]. A. Godlyn Abraham, A. Manikandan, E. Manikandan, S. Vadivel, S. K. Jaganathan, A. Baykal, P. Sri Renganathan, Enhanced magneto-optical and photo-catalytic properties of transition metal cobalt (Co^{2+} ions) doped spinel $MgFe_2O_4$ ferrite nanocomposites, J. Magn. Magn. Mater. 452 (2018) 380-388.

[5]. M. Maria Lumina Sonia, S. Anand, S. Blessi, S. Pauline, A. Manikandan, Effect of surfactants (PVB/EDTA/CTAB) assisted sol-gel synthesis on structural, magnetic and dielectric properties of $NiFe_2O_4$ nanoparticles, Ceram. Int. 44 (2018) 22068-22079.

[6]. K. Elayakumar, A. Dinesh, A. Manikandan, P. Murugesan, G. Kavitha, S. Prakash, R. Thilak Kumar, S. K. Jaganathan, A. Baykal, Structural, morphological, enhanced magnetic properties and antibacterial bio-medical activity of rare earth element (REE) Cerium (Ce^{3+}) doped $CoFe_2O_4$ nanoparticles, J. Magn. Magn. Mater. 476 (2019) 157-165.

[7]. Md Amir, H. Gungunes, A. Baykal, M. Almessiere, H. Sozeri, I. Ercan, M. Sertkol, S. Asiri, A Manikandan, Effect of annealing temperature on Magnetic and Mossbauer properties of $ZnFe_2O_4$ nanoparticles by sol-gel approach, J. Supercond. Nov. Magn. 31 (2018) 3347–3356.

[8]. I. J. C. Lynda, M. Durka, A. Dinesh, A. Manikandan, S. K. Jaganathan, A. Baykal, S. Arul Antony, Enhanced Magneto-optical and Photocatalytic Properties of Ferromagnetic $Mg_{1-y}Ni_yFe_2O_4$ ($0.0 \leq y \leq 1.0$) Spinel Nano-ferrites, J. Supercond. Nov. Magn. 31 (2018) 3637–3647.

[9]. M. Maria Lumina Sonia, S. Anand, V. Maria Vinosel, M. Asisi Janifer, S. Pauline, A. Manikandan, Effect of lattice strain on structure, morphology and magneto-dielectric properties of $NiGd_xFe_{2-x}O_4$ ferrite nano-crystallites synthesized by sol-gel route, J. Magn. Magn. Mater. 466 (2018) 238-251.

[10]. A. Godlyn Abraham, A. Manikandan, E. Manikandan, S. K. Jaganathan, A. Baykal, P. Sri Renganathan, Enhanced Opto-Magneto Properties of $Ni_xMg_{1-x}Fe_2O_4$ ($0.0 \leq x \leq 1.0$) Ferrites Nano-Catalysts, J. Nanoelect. Optoelect. 12 (2017) 1326–1333

[11]. S. Asiri, M. Sertkol, S. Guner, H. Gungunes, K.M. Batoo, T.A. Saleh, H. Sozeri, M.A. Almessiere, A. Manikandan, A. Baykal, Hydrothermal synthesis of $Co_yZn_yMn_{1-2y}Fe_2O_4$ nanoferrites: Magneto-optical investigation, Ceram. Int. 44 (2018) 5751–5759.

[12]. A. Baykal, S. Guner, H. Gungunes, K.M. Batoo, Md. Amir, A. Manikandan, Magneto Optical Properties and hyperfine interactions of Cr^{3+} ion substituted copper ferrite nanoparticles, J. Inorg. Organomet. Polym. 28 (2018) 2533–2544,

[13]. E. Hema, A. Manikandan, P. Karthika, M. Durka, S. Arul Antony, B. R. Venkatraman, Magneto-optical properties of recyclable spinel $Ni_xMg_{1-x}Fe_2O_4$ ($0.0 \leq x \leq 1.0$) nano-catalysts, J. Nanosci. Nanotech. 16 (2016) 7325-7336.

[14]. Y. Slimani, A. Baykal, Md. Amir, N. Tashkandi, H. Güngüneş, S. Guner, H.S. El Sayed, F. Aldakheel, T.A. Saleh, A. Manikandan, Substitution effect of Cr^{3+} on hyperfine interactions, magnetic and optical properties of Sr-hexaferrites, Ceram. Int. 44 (2018) 15995-16004.

[15]. Y. Slimani, H. Gungunes, M. Nawaz, A. Manikandan, H.S. El Sayed, M.A. Almessiere, H. Sozeri, S.E. Shirsath, I. Ercan, A. Baykal, Magneto-optical and microstructural properties of spinel cubic copper ferrites with Li-Al co-substitution, Ceram. Int. 44 (2018) 14242-14250.

[16]. S. Asiri, S. Güner, A. Demir, A. Yildiz, A. Manikandan, A. Baykal, Synthesis and Magnetic Characterization of Cu Substituted Barium Hexaferrites, J. Inorg. Organomet. Polym. Mater. 28 (2018) 1065–1071.

[17]. A. Silambarasu, A. Manikandan, K. Balakrishnan, Room temperature superparamagnetism and enhanced photocatalytic activity of magnetically reusable spinel $ZnFe_2O_4$ nano-catalysts, J. Supercond. Nov. Magn. 30 (2017) 2631–2640.

[18]. G. Padmapriya, A. Manikandan, V. Krishnasamy, S. K. Jaganathan, S. Arul Antony, Enhanced catalytic activity and magnetic properties of spinel $Mn_xZn_{1-x}Fe_2O_4$ ($0.0 \leq x \leq 1.0$) nano-photocatalysts by microwave irradiation route, J. Supercond. Nov. Magn. 29 (2016) 2141-2149.

[19]. S. Gunasekaran, K. Thanrasu, A. Manikandan, M. Durka, A. Dinesh, S. Anand, S. Shankar, Y.Slimani, M. A. Almessiere, A. Baykal, Structural, fabrication and enhanced electromagnetic wave absorption properties of reduced graphene oxide (rGO)/zirconium substituted cobalt ferrite ($Co_{0\cdot5}Zr_{0\cdot5}Fe_2O_4$) nanocomposites, Physica B: Condensed Matter, 605 (2021) 412784.

[20]. F. Hussain, S. Z. Shah, H. Ahmad, S. A. Abubshait, H. A. Abubshait, A. Laref, A. Manikandan, H. S. Kusuma, M. Iqbal, Microalgae an ecofriendly and sustainable wastewater treatment option: Biomass application in biofuel and bio-fertilizer production. A review, Renewable and Sustainable Energy Reviews, 137 (2021) 110603.

[21]. P. A. Vinosha, A. Manikandan, A. S. J. Ceicilia, A. Dinesh, G. F. Nirmala, A. Christy Preetha, Y. Slimani, M.A. Almessiere, A. Baykal, B. Xavier, Review on recent advances of zinc substituted cobalt ferrite nanoparticles: Synthesis characterization and diverse applications, Ceramics International, 47 (2021) 10512-10535.

[22]. S. Blessi, S. Anand, A. Manikandan, M. M. Lumina Sonia, V. Maria Vinosel, Y. Slimani, M.A. Almessiere, A. Baykal, Structural, optical and electrochemical investigations of Sb substituted mesoporous SnO_2 nanoparticles, Journal of Materials Science: Materials in Electronics, 32 (2021) 4132–4145.

[23]. Y. Slimani, N. A. Algarou, M. A. Almessiere, A. Sadaqat M. G. Vakhitov, D. S. Klygach, D. I. Tishkevich, A. V. Trukhanov, S. Güner, A. S. Hakeem, I. A. Auwal, A. Baykal,

A. Manikandan, I. Ercan, Fabrication of exchanged coupled hard/soft magnetic nanocomposites: Correlation between composition, magnetic, optical and microwave properties, Arabian Journal of Chemistry, 10 (2021) 102992.

[24]. P. Manimaran, S. Balasubramaniyan, M. Azam, D. Rajadurai, S. I. Al-Resayes, G. Mathubala, A. Manikandan, S. Muthupandi, Z. Tabassum, I. Khan, Synthesis, Spectral Characterization and Biological Activities of Co(II) and Ni(II) Mixed Ligand Complexes, Molecules, 26 (2021) 823.

[25]. O. Alagha, N. Ouerfelli, H. Kochkar, M. A. Almessiere , Y. Slimani, A. Manikandan, A. Baykal, A. Mostafa, M. Zubair, M. H. Barghouthi, Kinetic Modeling for Photo-Assisted Penicillin G Degradation of $(Mn_{0.5}Zn_{0.5})[Cd_xFe_{2-x}]O_4$ ($x \leq 0.05$) Nanospinel Ferrites, Nanomaterials, 11 (2021) 970.

[26]. M. R. Ranjitha, A. Manikandan, J. N. Baby, K. Panneerselvam, S. Ragu, Mary George, Y. Slimani, M.A. Almessiere, A. Baykal, Hexagonal basalt-like ceramics $La_xMg_{1-x}TiO_3$ (x = 0 and 0.5) contrived via deep eutectic solvent for selective electrochemical detection of dopamine, Physica B: Condensed Matter, 615 (2021) 413068.

[27]. M. A. Almessiere, B. Unal, I.A. Auwal, Y. Slimani, H. Aydin, A. Manikandan, A. Baykal, Impact of calcination temperature on electrical and dielectric properties of $SrGa_{0.05}Fe_{11.98}O_4$-$Zn_{0.5}Ni_{0.5}Fe_2O_4$ hard/soft nanocomposites, Journal of Materials Science: Materials in Electronics, 32 (2021) 16589-16600.

[28]. K. Geetha, R. Udhayakumar, A. Manikandan, Enhanced magnetic and photocatalytic characteristics of cerium substituted spinel $MgFe_2O_4$ ferrite nanoparticles, Physica B: Physics of Condensed Matter, 615 (2021) 413083.

[29]. S. S. Al-Jameel, S. Rehman, M. A. Almessiere, F. A. Khan, Y. Slimani, N. S. Al-Saleh, A. Manikandan, E. A. Al-Suhaimi, A. Baykal, Anti-microbial and anti-cancer activities of $MnZnDy_xFe_{2-x}O_4$ ($x \leq 0.1$) nanoparticles, Artificial Cells, Nanomedicine and Biotechnology, 49 (2021) 493-499.

[30]. S. Rehman, M. A. Almessiere, S. S. Al-Jameel, U. Ali, Y. Slimani, N. Taskhandi, N. S. Al-Saleh, A. Manikandan, F. A. Khan, E. A. Al-Suhaimi, A. Baykal, Designing of $Co_{0.5}Ni_{0.5}Ga_xFe_{2-x}O_4$ ($0.0 \leq x \leq 1.0$) Microspheres via Hydrothermal Approach and Their

Selective Inhibition on the Growth of Cancerous and Fungal Cells, Pharmaceutics, 13 (2021) 962.

[31]. M. A. Almessiere, B. Unal, Y. Slimani, H. Gungunes, M. S. Toprak, N. Tashkand, A. Baykal, M. Sertkol, A.V. Trukhanov, A. Yıldız, A. Manikandan, Effects of Ce-Dy rare earths co-doping on various features of Ni-Co spinel ferrite microspheres prepared via hydrothermal approach, J. of Materials Research and Technology, 14 (2021) 2534-2553.

[32]. S. Blessi, A. Manikandan, S. Anand, M. M. L. Sonia, V. M. Vinosel, P. Paulraj, Y. Slimani, M.A. Almessiere, M. Iqbal, S. Guner, A. Baykal, Effect of Zinc substitution on the physical and electrochemical properties of mesoporous SnO_2 nanomaterials, Materials Chemistry and Physics, 273 (2021) 125122.

[33]. M. A. Almessiere, Y. Slimani, Y. O. Ibrahim, M. A. Gondal, M. A. Dastageer, I. A. Auwal, A. V. Trukhanov, A. Manikandan, A. Baykal, Morphological, structural, and magnetic characterizations of hard-soft ferrite nanocomposites synthesized via pulsed laser ablation in liquid, Materials Science and Engineering B, 273 (2021) 115446.

[34]. S. Blessi, S. Anand, A. Manikandan, M. Maria Lumina Sonia, V. Maria Vinosel, Y. Slimani, M.A. Almessiere, A. Baykal, Influence of Ni substitution on opto-magnetic and electrochemical properties of CTAB capped mesoporous SnO_2 nanoparticles, Journal of Materials Science: Materials in Electronics, Journal of Materials Science: Materials in Electronics, 32 (2021) 7630–7646.

[35]. M. George, T.L. Ajeesha, A. Manikandan, Ashwini Anantharaman, R.S. Jansi, E. Ranjith Kumar, Y. Slimani, M.A. Almessiere, A. Baykal, Evaluation of Cu-$MgFe_2O_4$ spinel nanoparticles for photocatalytic and antimicrobial activates, Journal of Physics and Chemistry of Solids, 153 (2021) 110010.

[36]. S. S. Al-Jameel, M. A. Almessiere, F. A. Khan, N. Taskhandi , Y. Slimani, N. S. Al-Saleh, A. Manikandan, E. A. Al-Suhaimi, A. Baykal, Synthesis, Characterization, Anti-Cancer Analysis of $Sr_{0.5}Ba_{0.5}Dy_xSm_xFe_{8-2x}O_{19}$ ($0.00 \leq x \leq 1.0$) Microsphere Nanocomposites, Nanomaterials, 11 (2021) 700.